Solar Energy 198 (2020) 385–398

Contents lists available at ScienceDirect

Solar Energy

journal homepage: www.elsevier.com/locate/solener

Comparison of optimal oriented façade integrated solar cooling systems in Australian climate zones

Dan Wu[a,b], Lu Aye[b], Yanping Yuan[c,*], Priyan Mendis[b], Tuan Ngo[b]

[a] School of Architecture and Design, Southwest Jiaotong University, Chengdu 611756, China
[b] Renewable Energy and Energy Efficiency Group, Department of Infrastructure Engineering, Melbourne School of Engineering, The University of Melbourne, Vic 3010, Australia
[c] School of Mechanical Engineering, Southwest Jiaotong University, Chengdu 610031, China

ARTICLE INFO

Keywords:
Solar cooling
PV
Adsorption
Absorption
Organic Rankine cycle

ABSTRACT

Solar cooling technologies have been proven to have great potential for energy saving during cooling season. Meanwhile, glass has become one of the primary structural materials used in building construction since the middle of the 20th century. Although common glass adds to the aesthetic appeal of a building, it has serious drawbacks, such as creating heat traps, preventing natural ventilation and causing glare. Highly glazed façades would cause unwanted heat transmission from the ambient, which must be extracted to outside using an air-conditioning system. Internal heat resulting from façade configurations can be responsible for up to 45% of a building's cooling requirements. A façade integrated solar cooling system can simultaneously improve building's energy efficiency, utilise solar energy and still maintain a high level of architectural and aesthetic quality. This investigation presents a consistent approach for optimising and comparing façade integrated solar cooling systems in terms of technical and financial performance. Four systems (a vapour compression cycle (VCC) chiller driven by semi-transparent photovoltaics (STPV) arrays, a single-stage absorption chiller, an adsorption chiller and a vapour compression chiller coupled with organic Rankine cycle (ORC) driven by evacuated tube solar collectors) were assessed and compared with a conventional electric vapour compression chiller. The systems investigated were modelled in TRNSYS and the models were applied to predict performance parameters in various climate zones (seven cities) in Australia. The solar fraction (SF) and unit cooling cost (UCC) were the two parameters applied to quantify the technical and financial aspects of each solar cooling system in seven cities in Australia. It was found that among the systems investigated, the VCC chiller with STPV system has the highest SF (100% except in Darwin) and lowest UCC ($0.21 kWh_r^{-1}) for all seven cities in Australia. In general, due to the grid as a virtual storage, ORC-VCC system has higher SF (40% and 50%) and lower UCC (5% and 10%) compared with adsorption and absorption chiller respectively in subtropical and temperate climate zones.

1. Introduction

With the rapid development of the world, the energy consumption has caused a series of serious environmental problems. In 2020, the world annual energy demand capacity will reach 750 million kilowatts, in which around 40% is contributed by buildings (Xuan et al., 2017). Meanwhile, the market for space cooling systems has been growing, not only due to improved indoor comfort standards and affordability of them, but also due to concerns on global warming (Eicker et al., 2015; Hartmann et al., 2011). However, most conventional space cooling systems which use vapour compression cycle (VCC) chillers mainly rely on grid electricity supplies. In Australia, heating, ventilation and air-conditioning (HVAC) systems account for 70% of total energy usage in commercial buildings (Rahman et al., 2010). The government of Western Australia stated that energy consumption in commercial buildings contributes about 10% of national greenhouse gas (GHG) emissions (2011). It could be estimated that the HVAC systems in commercial buildings contribute approximately 7% of Australia's GHG emissions. It also has been reported that cooling demand in Australia is highly sensitive to global warming (Wang et al., 2010). To stabilise and slow the global warming, various renewable energy technologies have been investigated. Buildings should have good thermal performance envelopes and they should utilise renewable energy available onsite. Solar cooling system with façade integration has a potential to make the building envelope better thermally perform, and as well as to use non-depletable energy source.

* Corresponding author.
E-mail address: ypyuan@home.swjtu.edu.cn (Y. Yuan).

https://doi.org/10.1016/j.solener.2020.01.003
Received 25 February 2019; Received in revised form 14 December 2019; Accepted 2 January 2020

Nomenclature

Symbols

A	aperture area of solar collector (m^2)
G	solar irradiance (kJ)
G_s	absorbed solar radiation per unit area (W m^{-2})
$K_{\tau\alpha}$	incidence angle modifiers (–)
M	air mass modifier (–)
m	air mass (–)
PLF	part load factor (–)
PLR	part load ratio (–)
$\dot{Q}$	heat transfer rate (W)
R_b	ratio of beam radiation on a tilted plane to that on horizontal plane (–)
T	temperature (K)

Greek symbols

α	absorptance (–)
β	slope angle (°)
η	efficiency (–)
θ	incidence angle (°)
ρ	reflectance (–)
τ	transmittance (–)

Subscripts

amb	ambient air
b	beam solar radiation
d	diffuse solar radiation
eq	equivalent
g	ground surface
op	operating
u	useful

Acronyms

ALCC	annualised life cycle cost
GHG	greenhouse gas
HVAC	heating, ventilation and air-conditioning
ORC	organic Rankine cycle
PV	photovoltaics
SF	solar fraction
STPV	semi-transparent photovoltaics
UCC	unit cooling cost
VCC	vapour compression cycle

Australia has abundant solar radiation and land resources. Annual solar radiation falling on Australia is 58 ZJ, approximately equivalent to 10 000 times Australia's annual energy consumption (Geoscience Australia and ABARE, 2010). Moreover, cooling dominant locations usually have abundant solar radiation, which matches the cooling demand. Thus, it is an attractive and logic way to use solar energy to drive space cooling systems that will be able to reduce both peak electricity demand and GHG emissions. Interest in solar cooling began in the 1970s, when the energy crisis occurred (Qu et al., 2010; Zeyghami et al., 2015). Solar cooling is an application of solar energy for cooling purpose (Koroneos et al., 2010). It has been proved that solar cooling can save approximately 50% of the energy cost of conventional cooling in Mediterranean climate locations (Balaras et al., 2007). The solar cooling concept includes a wide range of cooling technologies driven by solar photovoltaic (PV) panels and solar thermal collectors, as illustrated in Fig. 1.

In solar cooling field, there are very rich literature resources available that focus on modelling, simulation optimisation and design

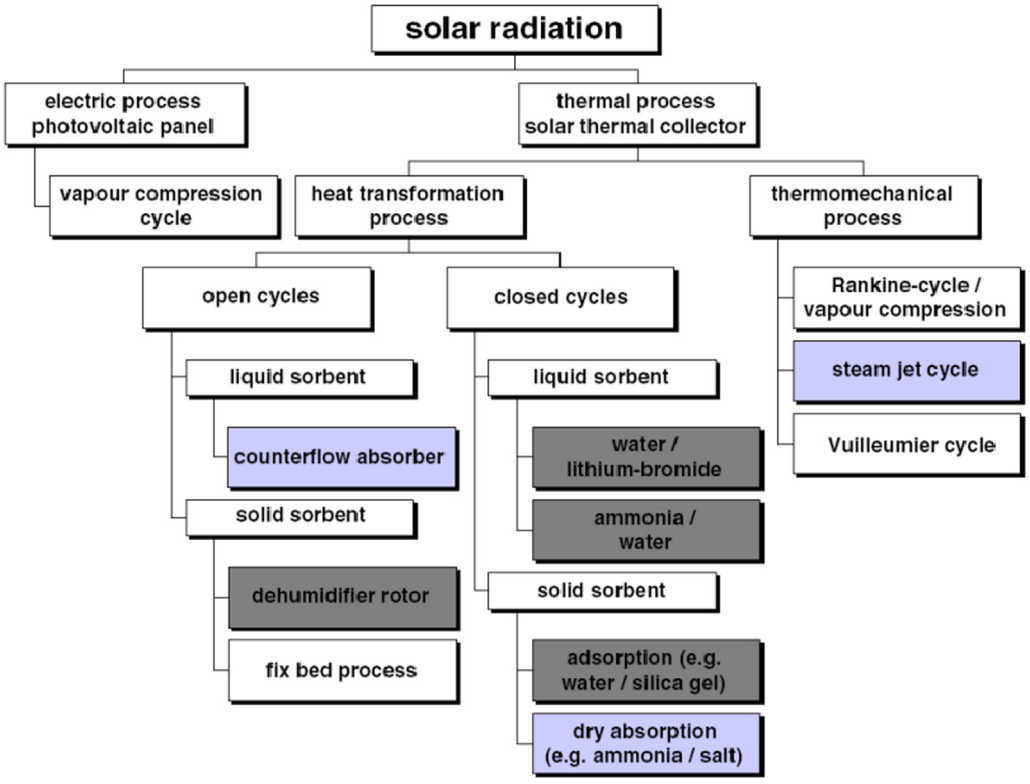

Fig. 1. Most common solar cooling technologies (Henning, 2007).

of various solar cooling technologies. There are numerous published review papers on a variety of solar cooling technologies. Allouhi et al. (2015) reviewed the feasibility of absorption, adsorption and ejector cooling systems. The study recommends that evacuated tube collectors are the best option for solar cooling and thermal energy storage, they efficiently improve the overall performance. Ullah et al. (2013) covered both solar PV and solar thermal systems, with a specific focus on solar sorption refrigeration systems with various working fluids. Earlier studies (Kim and Ferreira, 2008; Otanicar et al., 2012) reviewed technologies that could be applied for solar cooling in terms of both technical and economic aspects. Both studies followed a relatively simply analysis approach without considering several variables that could play key roles in the system operation. Lazzarin and Noro (2018) conducted a comprehensive review on a wide range of solar cooling technologies and concluded that situations favour PV driven technologies in terms of investment cost.

Although the solar cooling has been extensively studied in the past, most comprehensive investigations have mainly tended to focus on the cooling technology especially for sorption chillers (Bellos et al., 2016; Eicker and Pietruschka, 2009; Lu et al., 2013; Raja and Shanmugam, 2012; Saghafifar and Gadalla, 2016; Weber et al., 2014) rather than on the system as a whole. Only few published works that assessed and compared both solar electric and thermal cooling technologies as a complete system in a comprehensive systematic way. Eicker et al. (2015) compared solar PV cooling system with solar sorption cooling system by evaluating the overall performance in office buildings for various climate conditions worldwide. Beccali et al. (2014) conducted a comparison of solar thermal and PV cooling systems by using life cycle assessment that considers both environment impacts and energy consumptions. Mokhtar et al. (2010) analysed the techno-economic performance of 25 feasible solar cooling combinations by considering location specific conditions, system cost and component performance characteristics. They all have concluded that the PV grid connected cooling plant performed better than solar thermal cooling system. However, a new organic Rankine cycle (ORC)-vapour compression cycle (VCC) cooling system was not considered and fully utilised in comparisons and none of these previous works have developed façade integrated solar field and studied façade integration as a whole system. There is not much published work that applies a consist method to assess and compare both solar electric and thermal cooling system. The existing comparisons mainly utilise simplified approach without considering key variables that affect the system overall performance.

To address this knowledge gap, two types of façade integrated solar fields were developed and a consistent approach was applied for comparing building façade integrated solar cooling systems that were optimised in terms of orientations and configurations of solar field and capacity of solar driven chillers in the present study. Four solar cooling technologies were selected and assessed in this investigation and compared with the conventional VCC cooling system which uses a scroll compressor for the chiller. One selected solar electric cooling system is driven by façade integrated PV modules and the other three solar thermal cooling systems driven by façade integrated evacuated tube solar collectors. The solar fraction (SF) and unit cooling cost (UCC) are the two parameters applied to quantify technical and financial aspect of each solar cooling system in seven cities of Australia. The feasible façade integrated solar cooling systems would be identified and recommended.

2. Method applied for systematic comparison

In this investigation, cooling systems for an office building were investigated for seven cities in Australia, including Darwin (12.45°S, 229.13°W), Brisbane (27.42°S, 206.92°W), Perth (31.93°S, 244.03°W), Sydney (33.93°S, 208.83°W), Adelaide (34.97°S, 221.47°W), Canberra (35.32°S, 210.8°W) and Melbourne (37.83°S, 215.25°W). The selected cities cover tropical, subtropical and temperate climate zones. All selected cooling systems were applied in each city and assessed individually with a consistent approach. A solar cooling system consists of a façade integrated solar field, a chiller and a working fluid for coolness transport. The comparison method considers solar radiation availability, building cooling load, façade integration, system performance parameters, component life time and costs of components. To compare the potential solar cooling technologies under certain weather conditions, two parameters SF and UCC were applied. The overall cooling

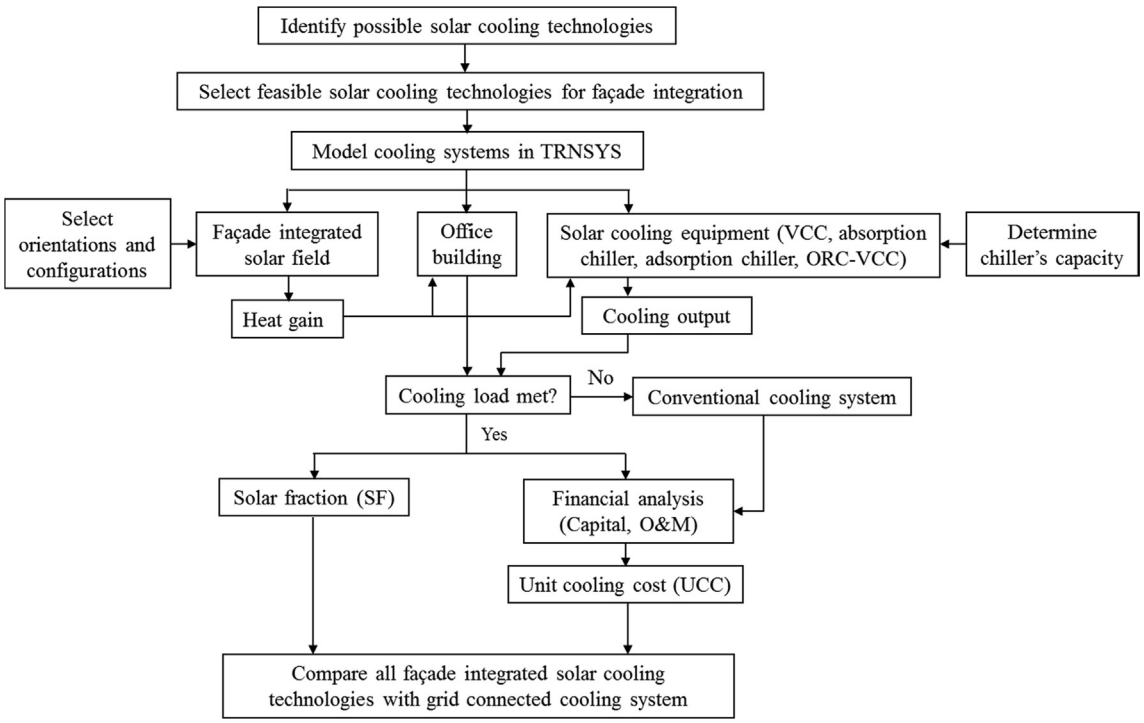

Fig. 2. Framework applied in assessing façade integrated solar cooling technologies.

system performance is assessed by using SF, which is the ratio between the load taken by solar and the total cooling load. UCC represents the present value of the life cycle cost paid for 1 kWh of cooling effect. Fig. 2 outlines the procedure used in evaluating SF and UCC.

The first step is to identify all commonly available solar cooling technologies on the market. According to façade integration requirements, the feasible solar cooling systems are selected afterwards. Besides solar cooling systems, a conventional grid connected chiller is also assessed as the baseline. The feasible combinations for façade integrated solar cooling technologies are briefly described in Section 3. After that, each selected system and conventional chiller are modelled in TRNSYS (Klein et al., 2010). The detailed modelling and technical design aspects are discussed in Section 4. According to previous findings, storage and backup components make significant contributions to initial annualised life cycle cost (ALCC) (Wu et al., 2013). Therefore, in this investigation, the systems were configured without heat storage tanks and battery banks. The cooling load is shared by both solar and conventional cooling systems. Conventional systems operate whenever the solar cooling system cannot meet the cooling demand. In addition, orientations and configurations of solar field and capacity of solar driven chillers are the key parameters that could affect system performance and they were considered in this investigation as discussed in the later section. Then, energy flows of each component were computed and used to compare system performance in SF and financial performance in UCC.

3. Façade integrated solar cooling technologies

As shown in Fig. 1, solar cooling can be mainly classified into solar electric and solar thermal. Solar electric cooling uses PV modules to produce electricity and an electric motor to drive the compressor of the conventional VCC. Solar thermal cooling uses solar collectors to collect thermal energy and a heat driven chiller to generate cooling effect. The most commonly used ones are listed in Table 1. The design of the proposed façade integration system not only allows the conversion from incoming solar radiation into electricity or useful heat, it also can reduce the indoor heat gain, without blocking visible light transmittance. The desirable characteristics of the solar field to be integrated with the building façade are:

- allowing occupants to see the outside view through the façade; and
- keeping low operating temperatures within the safe range to prevent façade damage from extreme temperatures

The flat plate collector (FPC) and parabolic trough collector (PTC) options were eliminated since they obstruct the outside view. The PTC requires tracking components which is also not feasible for façade integration. For the same reason, building integrated with concentrating photovoltaic (BICPV) technology was not considered in this study although it could reach 17% efficiency (Guiqiang et al., 2014). The double-stage absorption chiller option, which requires a generation temperature higher than 120 °C, was also excluded to avoid extreme façade temperatures. Desiccant cooling systems require relatively high humidity air. The selected cities in this study do not have high air relative humidity issues. Therefore, four feasible solar cooling technology combinations were identified. They are:

- façade integrated semi-transparent PV (STPV) coupled with VCC chiller;
- façade integrated ETC with combined ORC and VCC chiller;
- façade integrated ETC with single-stage absorption chiller, and
- façade integrated ETC with adsorption chiller.

Water is selected as the working fluid in ETCs due to its higher volumetric specific heat capacity than that of air. Low volumetric specific heat capacity of air requires high volume flow rate that would increase the system cost.

3.1. Façade integrated solar field

In this investigation, natural ventilated façade integrations were adopted for both STPVs and ETCs. The STPVs and ETCs are placed in front of sealed double-glazing façades. Low-e and reflective glass is used for the back double-glazing curtain wall. The cavity between the STPVs/ETCs and the back double-glazing was assumed to be fully ventilated. The solar field covers the full façades to maximise the solar collection.

The STPV module is made up of opaque mono-crystalline cells with transparent space in between. Besides PV cells, the module also consists of glass and encapsulation material (Ethylene Vinyl Acetate (EVA sheet)). This type of PV panels not only can produce electricity it also allows light transmission through the transparent part. In the meantime, lower solar heat gain is achieved by blocking solar radiation from the solar cells. The structure of STPV is shown in Fig. 3. The front and back glass cover of STPV is low-iron tempered glass. The thermal performance of STPV is mainly determined by orientation, efficiency of solar cells, solar cell area ratio and module thickness. The larger solar cell area in the STPV panels can increase electricity generation and reduce more heat gain but with less light transmission. Thus, a balance between electricity generation, daylight transmission and solar heat gain should be found. According to Fung & Yang's study (2008), 70% reduction of solar heat gain can be obtained when the solar cell area ratio is 0.8. Since STPV is one of the most promising façade integrated technologies for power generation, many researches have focused on its energy performance, heat transfer and fluid flow behaviour (Gan, 2009; Guardo et al., 2009; Infield et al., 2006; Miyazaki et al., 2005; Radhi, 2010; Song et al., 2008; Wang et al., 2006).

In a solar thermal cooling system, solar energy is collected by solar collectors and used in a thermo-chemical or a thermo-mechanical device to produce cooling. Advanced ETC is able to heat water to about 160 °C. It can provide the required temperature heat source for single-stage absorption chiller, adsorption chiller and ORC. The spacing between each tube allows light transmission through the façade. A tube layout for the integrated façade of the building is illustrated in Fig. 4. The front glass cover provides protection for ETCs against unexpected external impact and bad weather to lower the maintenance cost.

3.2. Solar cooling systems

The proposed façade solar electric, single-stage absorption chiller,

Table 1
Optional solar cooling components (Note: the shaded entries are not suitable) (adapted from AIRAH, 2018).

Solar	Cooling	Delivery	Comment
Photovoltaic (PV)	Electric motor vapour compression cycle (VCC)	Air	Electricity generated when cooling not required
Evacuated tube collector (ETC)	Organic Rankine cycle (ORC) + vapour compression cycle	Water	Electricity generated when cooling not required
	Absorption chiller (single-stage)		Cooling only, environment issue
	Adsorption chiller		Cooling only, long lifetime
Parabolic trough collector (PTC)	Absorption chiller (double-stage)		
Flat plate collector (FPC)	Desiccant		

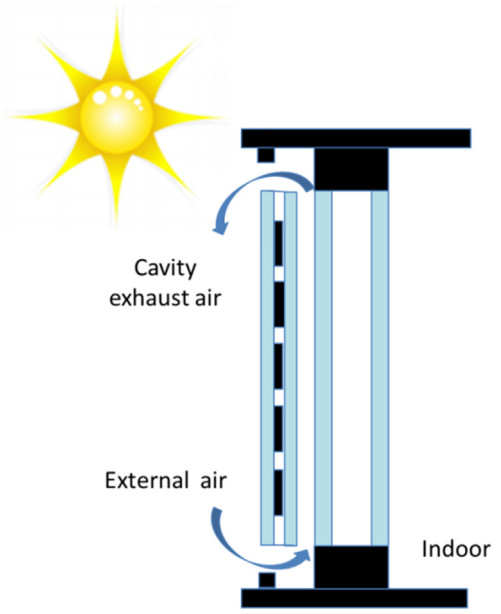

Fig. 3. Layout of a façade integrated STPV.

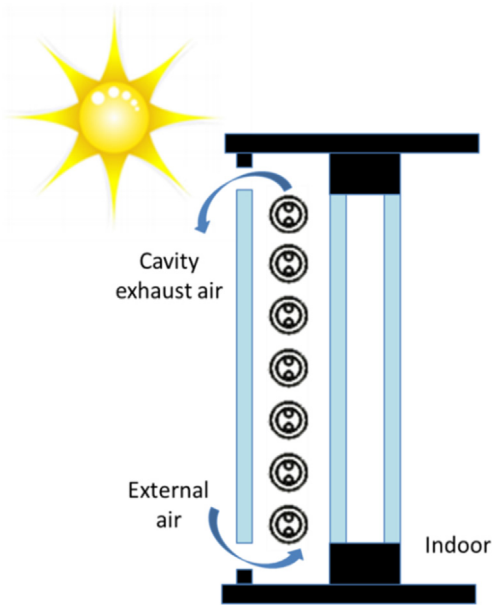

Fig. 4. Layout of a façade integrated ETC.

adsorption chiller and ORC-VCC cooling system investigated are presented in Figs. 5–8.

As a newly developed solar cooling system, ORC coupled with a VCC chiller system is a thermo-mechanical cooling technology. Fig. 8 illustrates how system components are connected. The main components are façade integrated ETCs, a buffer tank, an ORC with recuperator, a water-cooled scroll type VCC chiller, a cooling tower, pumps and an electric generator.

The detailed working principle and process have been described in the first author's previous work (Wu et al., 2017). It should be noted that the proposed system is a formulated concept. The efficiency of ORC is about 10% and the compressor COP of the scroll type vapour compression chiller is typically at least 4. The compressor COP is defined as the ratio between refrigerant effect and the compressor power input. The working fluid of the power cycle and cooling cycle is R134a. In reality it may not be always the case, different working fluids could be used for ORC and VCC. Although R134a is selected for both cycles, the operating conditions of each cycle are independent. Therefore, each cycle can optimise based on its own characteristics to achieve better performance. This is because the ORC is less sensitive to the condensing temperature than is in the VCC chiller (Wang et al., 2011). Keeping the refrigerant separate also allows different lubricants to be used in each cycle corresponding to different operating conditions in the expander and compressor.

4. Modellings and simulations

As the proposed system performance is expected to be transient, computer modelling is necessary to understand its performance. The system performance was evaluated and the annual solar fractions were estimated for each solar cooling system in seven cities in Australia as mentioned in Section 2. TRNSYS simulation studio was used to model the proposed system over small-time increments, in which its major components were represented by the standard and TESS Types. The flow chart (Fig. 9) presents the modelling procedure. Typical Meteorological Year (TMY) weather data (Morrison and Litvak, 1999) was applied, which has been proven to provide a reliable estimation for a wide range of solar thermal systems over a long term average annual performance of. TMY data and part-load performance are the input for this model. The cooling load from a building simulation is used in system simulation to generate time series and annual results. Time series results include energy flow at each time step used in technical performance analysis. Hourly time step was applied to avoid "stair-step" effect (Delcroix et al., 2012).

4.1. Building description

The building selected is a two-story office building recommended by the Australia Building Codes Board (ABCB) to represent a typical office building mostly found in the CBD of Australia (ABCB, 2001). The building has total floor area 3000 m^2 and two sides of the building are covered by either façade integrated STPV or façade integrated ETCs as illustrated in Figs. 3 and 4 respectively. Double glazing façades (overall heat transfer coefficient: 0.86 W m^{-2} K^{-1}, solar heat gain coefficient: 0.598 and visible transmittance: 0.706) are installed on the south and east sides of the building without a solar field. The walls are constructed mainly with concrete. The U-factor of ground level floor, top level floor, roof and exterior wall are 1.438, 1.419, 0.193 and 0.371 W m^{-2} K^{-1} respectively.

Type 56 was used to model the building. Each floor was considered as one zone in the model, due to the relatively small building size. Moreover, the main purpose of this building simulation is to estimate the total cooling load not the temperature distribution. The daily occupancy, thermal setting were given in previous study (Wu et al., 2013). The properties of the building envelope were defined to meet National Construction Code (NCC) requirements in each city. Infiltration rate (0.6 ACH), ventilation rate (0.3 ACH), cooling setting temperature (24 °C), internal gains (36 people seating and doing light work during office hours (9 am to 5 pm), 140 W per computer and 10 Wm^{-2} artificial lighting with a 40% convective part) were assumed. The cooling schedule started one hour earlier and ended one hour later than occupancy hours.

4.2. Façade integrated STPV

The PV module is thin and large compared with its lateral dimensions. Therefore, one-dimensional heat transfer model can be applied. Regarding the structure of the STPV panel, the panel area consists of both opaque solar cells and transparent part. The heat transfer through the STPV panel can be divided into two parts: opaque and transparent. In the opaque part, solar radiation is absorbed by solar cells after passing through the front glass. The front glass cover contacts outdoor

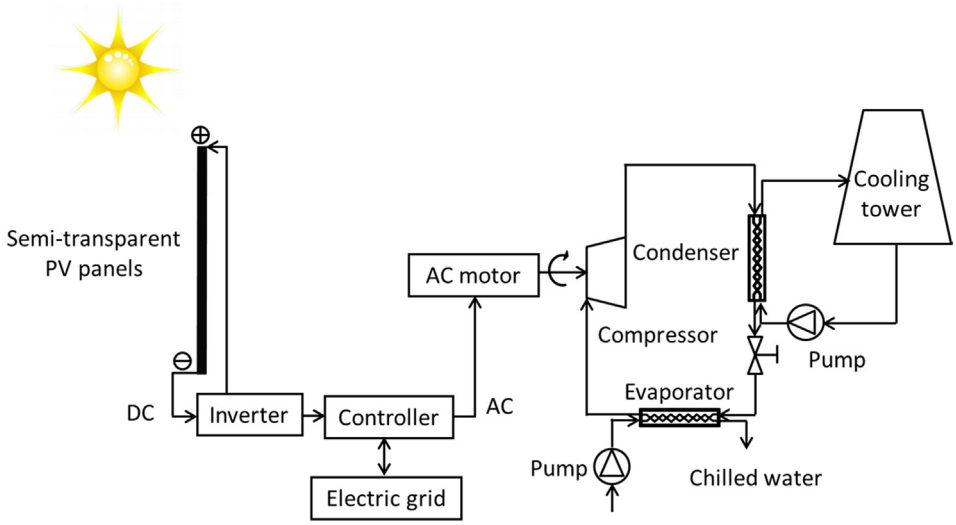

Fig. 5. Schematic of the façade integrated solar electric cooling system.

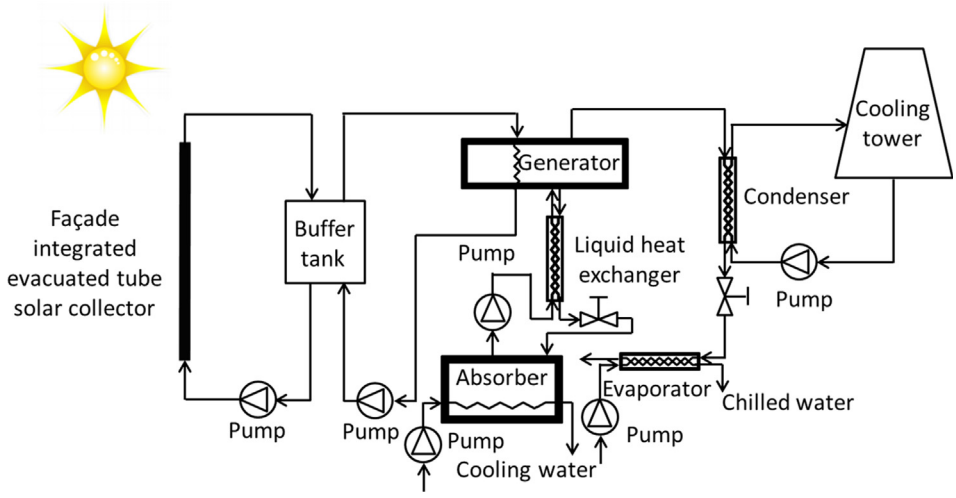

Fig. 6. Schematic of the façade integrated solar single-stage absorption cooling system.

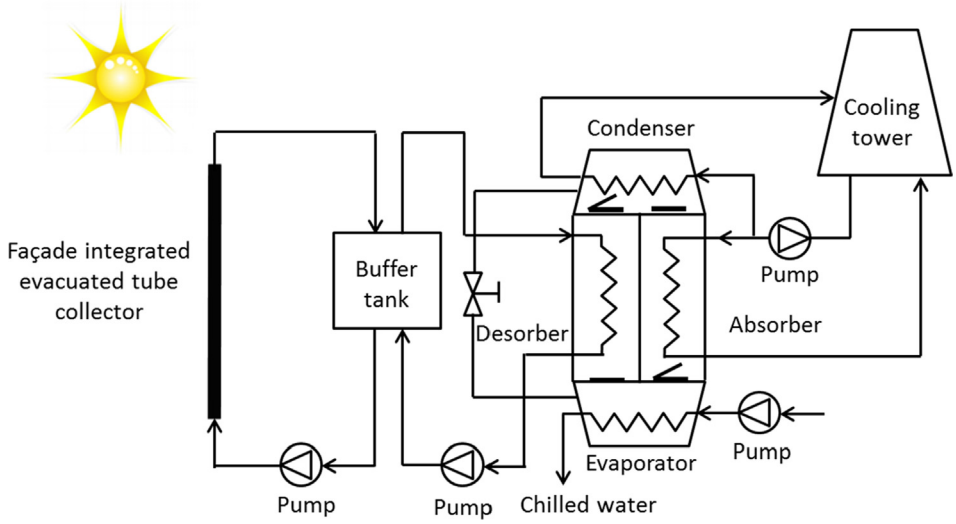

Fig. 7. Schematic diagram of the façade integrated solar adsorption cooling system.

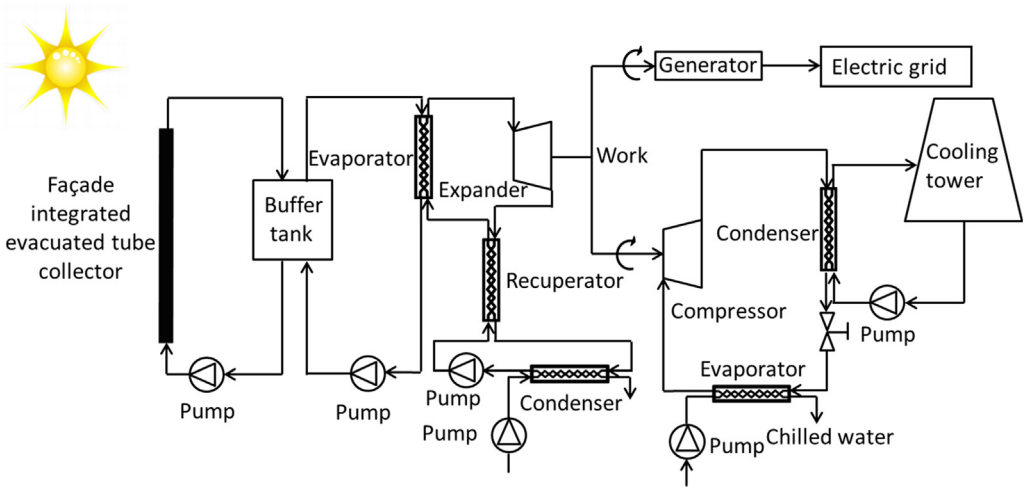

Fig. 8. Schematic diagram of the façade integrated ETC-ORC-VCC system.

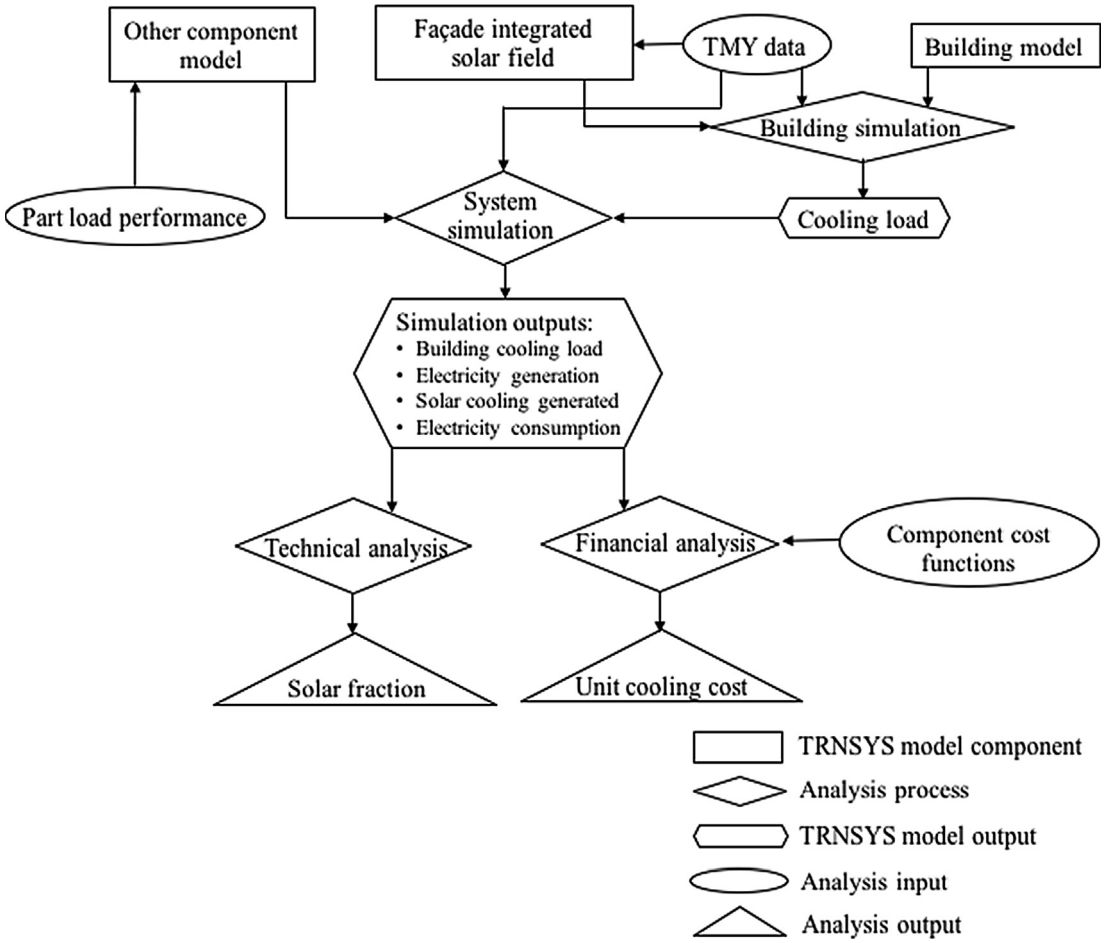

Fig. 9. TRNSYS modelling flow chart.

environment and also absorbs part of the solar radiation. The absorbed heat is released towards both the front and back (Lu and Law, 2013). For the transparent part, most of the solar radiation transmitted to the back, in which a small amount of heat is also absorbed by the glass and released gradually. The absorbed heat is exchanged with the outside environment by means of convection and radiation. The double-glazing façade at the back is included in the building model. In this model, solar radiation that is reflected, absorbed and transmitted at each layer is considered from both optical and thermal perspectives. The heat loss from STPV does not directly affect the indoor environment due to full ventilation. However, the transmitted solar radiation through STPV is contributing to the building's cooling load which needs to be considered.

TESS library Type 562 was used to model the solar cell part of the module including glass covers to evaluate the total power generation from the STPV panel and efficiency of the PV module. In this model, the instantaneous overall efficiency changes with cell temperature and incident solar radiation. The efficiency at the reference conditions,

Table 2
Properties of the STPV module.

Properties	Values
Cell area ratio	0.85
Absorptance of solar cell	0.9
Emittance of glass cover	0.86
Glass cover thickness (mm)	6
Glass cover conductivity (kJ h^{-1} m^{-1} K^{-1})	6.48
Refractive index of glass cover	1.5
Solar cell efficiency at reference condition	16%
Reference temperature (°C)	25
Reference radiation (kJ h^{-1} m^{-2})	3600
Efficiency modifier for temperature (C^{-1})	−0.0045
Efficiency modifier for radiation (hm^2 kJ^{-1})	0.0000025

coefficients that describe how efficiency changes with the cell temperature and incident solar radiation, need to be provided as known parameters. The properties of the modelled STPV are listed in Table 2. The power generation is mainly dependent on the absorbed solar radiation, which is determined by incident radiation, air mass and incident angle. Since solar radiation data on the vertical plane is not directly available, it is necessary to estimate it by using the horizontal solar radiation data and incidence angle at each time step.

Unlike a flat plate solar collector, the spectral effect is considered in modelling the performance of PV modules. The absorbed solar radiation can be obtained from Eq. (1) (Duffie and Beckman, 2013).

$$G_s = (\tau\alpha)_n M\left(G_b R_b K_{\tau\alpha,b} + G_d K_{\tau\alpha,d}\frac{1+\cos\beta}{2} + G\rho_g K_{\tau\alpha,g}\frac{1-\cos\beta}{2}\right) \quad (1)$$

where G_s is the absorbed solar radiation per unit area (Wm^{-2}), $(\tau\alpha)_n$ is the product of transmittance and absorptance, M the is air mass modifier, G_b, G_d and G are the beam, diffuse and total irradiance (Wm^{-2}), R_b is the ratio of beam radiation on a tilted plane to that on horizontal plane, $K_{\tau\alpha,b}$, $K_{\tau\alpha,d}$ and $K_{\tau\alpha,g}$ are the incidence angle modifiers at the beam incidence, diffuse and ground-reflected radiation, β is slope angle of the PV (°) and ρ_g is ground reflectance.

Eq. (2) is an empirical relation developed by King et al. (2004) accounts for changes in the spectral distribution due to changes in the air mass.

$$M = \alpha_0 + \alpha_1 m + \alpha_2 m^2 + \alpha_3 m^3 + \alpha_4 m^4 \quad (2)$$

where m is air mass, $\alpha_{0\ldots4}$ are coefficients. There are different values for different PV cell materials. For monocrystalline cells, these values are 0.935823, 0.054289, −0.008677, 0.000527 and −0.000011 respectively (Davis et al., 2002). R_b is given by Eq. (3).

$$R_b = \frac{\cos\theta}{\cos\theta_z} \quad (3)$$

where θ is the incidence angle for beam radiation (°) and θ_z is the solar zenith angle (°). The incidence angle modifier also can be obtained from an empirical relation developed by King et al. (1997) in Eq. (4).

$$K_{\tau\alpha} = b_0 + b_1\theta + b_2\theta^2 + b_3\theta^3 + b_4\theta^4 + b_5\theta^5 \quad (4)$$

where $K_{\tau\alpha}$ is the incidence angle modifier, $b_{0\ldots5}$ are constants. $K_{\tau\alpha}$ represents beam, diffuse and ground radiation by substituting different values of θ. The $b_{0\ldots5}$ values for monocrystalline cells are 1.000341, −0.005557, 6.553×10^{-4}, -2.703×10^{-5}, 4.641×10^{-7} and -3.371×10^{-9} (Davis et al., 2002). In this study, the constant values for the effective incidence angles are provided by Duffie and Beckman (2013) as shown in Eqs. (5) and (6).

$$\theta_{e,d} = 59.68 - 0.1388\beta + 0.001497\beta^2 \quad (5)$$

$$\theta_{e,g} = 90 - 0.5788\beta + 0.002693\beta^2 \quad (6)$$

where $\theta_{e,d}$ and $\theta_{e,g}$ are the effective incidence angles for diffuse and ground reflected radiation respectively (°).

The transparent part is made of three layers, including front glass, bank glass and resin, which is a viscous transparent substance filling the gap between the two glass covers. The width of the gap is in the order of 300–800 μm, which is negligible compared with the thickness of the glass (Fung and Yang, 2008). The transmittance of the resin layer was assumed to be 0.9 as a constant since its thickness is negligible. The solar radiation that passes through the transparent part is a function of the transmittance of each layer and incidence angle modifier can be calculated using Eq. (4).

4.3. Façade integrated ETC

The modelling concept for ETCs is similar to that for STPV. The energy balance model can be divided into opaque and transparent parts. Due to the fully ventilated cavity, the front cover glass, ETCs and double-glazing back panel were also modelled separately. The modelling of back double glazing is same as the one explained in Section 4.2. The heat loss from ETCs also does not affect the inside building environment. However, the transmitted solar radiation through front glazing contributes to the building cooling load. The equivalent normal radiation (G_{eq}) transmitted through the front cover is determined by correlations (Eqs. (7)–(10)) provided by (Bosanac and Nielsen, 1997).

$$G_{eq} = K_{\tau\alpha,b}G_b + K_{\tau\alpha,d}G_d + K_{\tau\alpha,g}G_g \quad (7)$$

where $K_{\tau\alpha,b}$, $K_{\tau\alpha,d}$ and $K_{\tau\alpha,g}$ are the incidence angle modifier for beam, diffuse and ground respectively, G_b, G_d and G_g are beam, diffuse and ground reflected radiation.

Where

$$K_{\tau\alpha,b}(\theta) = 1 - \left[\tan\left(\frac{\theta}{2}\right)\right]^{1/r} \quad (8)$$

$$K_{\tau\alpha,d}(\theta) = 2\int_0^{\pi/2}\left[1 - \left[\tan\left(\frac{\theta}{2}\right)\right]^{1/r}\right]\sin(\theta)\cos(\theta)d\theta \quad (9)$$

$$K_{\tau\alpha,d} = K_{\tau\alpha,g} \quad (10)$$

where θ is the incidence angle and $r(0.24)$ is the coefficient for fitting the incidence angle modifier derived from transitivity with different incidence angle.

A commercially available ETC was used in the simulation. The specifications of an ETC array based on the gross area are summarised in Table 3. Type 71 was used to model the ETC array to evaluate the solar energy from the transmitted solar radiation. The total useful energy gained of the ETC is found from Eq. (11) (Duffie and Beckman, 2013).

$$\dot{Q}_u = A(G\ K_{\tau\alpha}\ \eta_o - C_1(T_{amb} - T_{op}) - C_2(T_{amb} - T_{op})^2) \quad (11)$$

where $\dot{Q}_u$ is useful energy gain (W), A is the aperture area of the collector (m^2), G is the total irradiation on the per unit area surface (W m^{-2}), $K_{\tau\alpha}$ is the incident angle modifier (IAM), η_0 is the optical efficiency of the collector, C_1 and C_2 is the performance coefficient, T_{amb} and T_{op} is ambient and average operating temperature (°C). IAM represents the correlations of both transmittance and absorption with the

Table 3
Specifications of the ETC (SPF, 2004).

Parameter	Value
Total length (m)	1.68
Width (m)	0.781
Absorber material	Copper
Absorber area (m^2)	1.938
Maximum operation pressure (kPa)	600
Intercept efficiency (–)	0.498
Negative of first order efficiency coefficient (W K^{-1} m^{-2})	1.61
Negative of second order efficiency coefficient (W K^{-2} m^{-2})	0.0027

angle of incidence. The used longitudinal and transverse IAM data was provided by the manufacturer. The total irradiation is calculated by Eq. (12). (Duffie and Beckman, 2013).

$$G = (G_b + G_d A)R_b + G_d(1 - A)\left(\frac{1 + \cos(\beta)}{2}\right) + G\rho_g\left(\frac{1 - \cos(\beta)}{2}\right) \quad (12)$$

where G_b, G_d and G are beam, diffuse and total radiation (W m^{-2}), R_b is the ratio of beam radiation on a tilted plane to that on a horizontal plane given by Eq. (2), β is the slope angle of the ETC (°) and ρ_g is ground reflectance. The shading caused by the adjacent collector tubes or PV cells will affect the solar radiation received on the inner double glazing. In this study, the shading effect of the ETCs and PV cells on the double glazing was taken into consideration by introducing a shading factor. Under current design, the internal glass panel will be exposed to the transmitted beam radiation when the incidence angle is between 0° and 31°. The shading factor varies with the incidence angle.

4.4. Cooling equipment

All chillers investigated in this study were water-cooled chillers, which are more common than air-cooled ones for large scale applications. Heat source inlet temperature, COP of chillers, and efficiency of the ORC were considered as dominant factors that influence system performance and were considered in the models. These parameters were based on the manufacturer's specifications as provided by Thermax, Makyekawa and Infinity. The supplied hot water temperature was assumed to be 75 °C, 90 °C and 85 °C for adsorption, absorption and ORC respectively. The rated COPs for the conventional vapour compression chiller, single-stage absorption chiller and adsorption chiller were assumed to be 3.6, 0.7 and 0.7 respectively. The efficiency of the ORC and the COP of directly coupled VCC chiller was assumed to be 12% (75 °C evaporating temperature, 30 °C condensing temperature) and 4.0 (72 °C evaporating temperature, 28 °C condensing temperature) respectively. The performance of a chiller varies with the cooling load. The part load and part load COP are correlated by using the part load ratio (PLR) and part load factor (PLF) as defined in Eqs. (13) and (14).

$$PLR = \frac{\text{Load}}{\text{Available full load capacity}} \quad (13)$$

$$PLF = \left[\frac{\text{Partial load efficiency}}{\text{Full load efficiency}}\right]_{\text{ORC}} = \left[\frac{\text{Partial load COP}}{\text{Full load COP}}\right]_{\text{chiller}} \quad (14)$$

The assumed part load factor curves for the ORC and chillers investigated are shown in Fig. 10. The original performance data for the chillers were provided by Koeppel et al. (1995), Henning (2007), Johnson Controls (2018) and Le et al. (2004). The ORC part load performance is derived from literature reported by Obernberger et al. (2002), in which the turbine speed is reduced at part load. The power required to run a wet cooling tower is dependent on the amount of heat rejected and the efficiency of the cooling tower at different ambient temperatures. The estimated power consumption is based on the manufacturer's data from Superchill (2018).

5. Preliminary system optimisation

5.1. Effect of façade orientations

Solar field orientation is one of the most critical factors that determines the system performance. The best orientations for PV and ORC systems can be found by evaluating annual total solar radiations on the vertical surface in various orientations since all useful heat gained will be used for either cooling or electricity generation. The solar radiation received on the vertical surface face for eight orientations [N (0°), NW (45°), W (90°), SW (135°), S (180°), SE (225°), E (270°), NE (315°)] for seven cities in Australia were estimated based on the TMY data. Since the floor plan of the building is square, the maximum number of potential orientations is four for each rotation. The northeast and northwest orientations have the highest annual total solar radiation for all cities except Darwin (see Fig. 11). If solar fields are located along these two orientations, the annual total solar radiation falling on the façade will be 10.68 GJ m^{-2}, 8.72 GJ m^{-2}, 8.27 GJ m^{-2}, 8.80 GJ m^{-2}, 8.70 GJ m^{-2} and 7.32 GJ m^{-2} for Brisbane, Perth, Sydney, Adelaide, Canberra and Melbourne respectively. For Darwin, the best orientation combination is north and west with 9.02 GJ m^{-2} the annual total solar radiation.

Not like PV and ORC systems, sorption chillers can generate only cooling effects (i.e. no electricity generation). No storage component was considered to store collected heat as mentioned in Section 2. Therefore, all excess solar energy will be wasted when cooling is not required. The actual cooling generation from solar energy is equal to the smaller of total building cooling load and total generated solar cooling. The solar sorption chillers were simulated for the cooling season, which was determined by the cooling degree day (CDD see Table 4). The cooling season applied for each city is shown in Table 5.

The best orientations for ETCs in sorption chiller systems cannot be determined by simply comparing total solar radiation falling on the tubes. Instead, the orientation selection is based on the overall system performance that is assessed by using the SF. The highest SF not only depends on solar radiation availability, it also depends on solar collector configuration and cooling load met by the solar cooling system. The detailed discussions on performance evaluations are presented in Section 5.2. Similarly, eight orientations were selected that generated 12 combinations of orientations. Since south side orientations receive about 10 times less solar radiation than other sides, it was not considered in the combinations. Fig. 12 shows solar fractions for 9 orientation combinations in seven cities for adsorption chiller systems. Except Darwin, combined northwest and northeast orientations is the best combination for other cities. In Darwin, the combined north and west orientations is the best combination for obtaining the highest SF. The same trend was observed for systems with single-stage absorption chillers. It should be noted that for sorption systems, the annual total solar radiation received is the criteria for façade orientations selection.

5.2. Effect of system size

The size of each component depends on the building's peak cooling load and the desired solar fraction to be achieved. Not like stand-alone systems, the maximum solar field area is fixed due to the limited façade area (240 m^2 on two sides of the building). The SF is the parameter used to assess the performance of each solar cooling system. However, the size of the solar field is not a fixed value. That is because the SF could reach 100% without utilising the full façade area for PV cooling application. The capacity of each chiller was taken as the peak cooling

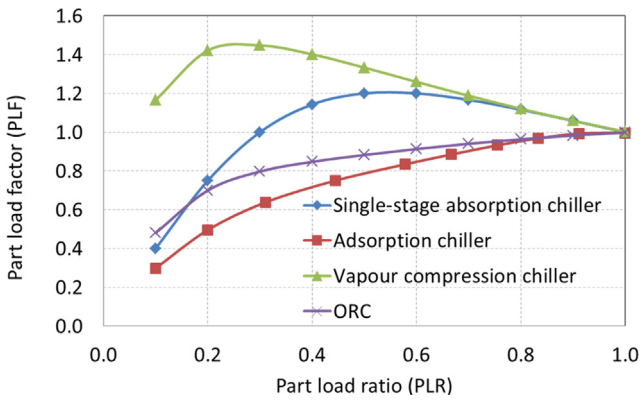

Fig. 10. Part load factor curves.

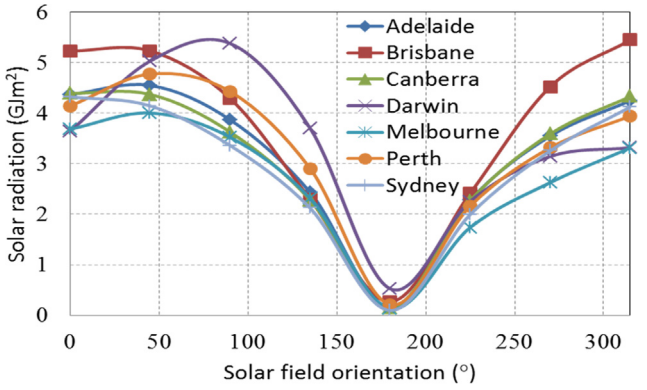

Fig. 11. Comparison of yearly total radiation falling on a vertical surface for seven cities.

load in this investigation for simplicity. In the SF calculations, ORC and PV systems use energy ratio due to electricity generation. In contrast, only cooling will be generated from sorption chillers. Therefore, the SF is taken as supplied cooling ratio.

To maximise the SF, configurations (no. of modules in series) of ETCs and capacity of solar driven chiller should be optimised for each system. Not like ORC systems, the orientation of ETCs in sorption systems cannot be determined from the beginning. Thus, the system optimising process is different as shown in Fig. 13. The peak cooling load is determined by using TRNSYS Type 56.

The main difference is the sequence of steps. The same processes were repeated for seven cities. Table 6 summarises the cooling load, optimal configurations of the solar field and the component size for the seven cities investigated. The building cooling reduces due to PV or ETC installation. Based on these design parameters, the simulated system electricity consumption is shown in Table 7.

6. Comparative assessment of façade integrated solar cooling systems

From the preliminary performance study, the design parameters of each façade integrated solar cooling system were determined. And their electricity consumption was generated accordingly. By using façade integrated solar field, both the peak cooling load and annual cooling demand are decreased in all cities, which leads to smaller capacity of chillers. For convenience, both façade share the same configurations of ETCs. Due to the high efficiency of PV system, except in Darwin (tropic climate), PV panels in other cities do not cover the façade fully to achieve 100% SF.

6.1. Financial performance

High investment cost has been identified as one of the main market barriers for solar cooling systems (Desideri et al., 2009). To make long-term decisions, it is essential to take into account life cycle costs (capital, operation and maintenance). This is particularly relevant for renewable energy systems that generally have higher initial cost and

Table 5
Cooling season assumed for seven cities.

City	Darwin	Brisbane	Perth	Sydney	Adelaide	Canberra	Melbourne
Begin	Jul	Aug	Sep	Sep	Oct	Nov	Oct
End	Jun	Jun	May	Apr	Apr	Mar	Apr

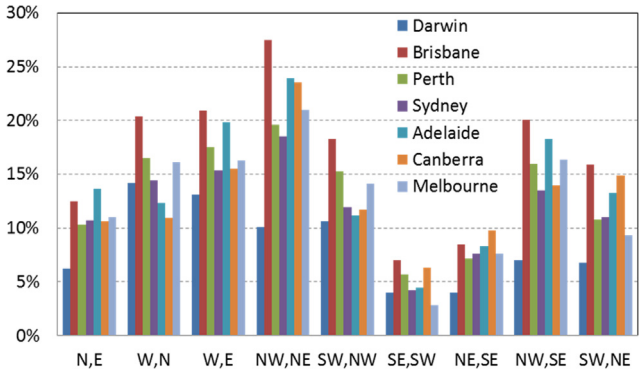

Fig. 12. Effect of orientation combinations on solar fraction for adsorption chiller system.

lower operating cost. The total cost of a cooling system includes equipment costs, design and installation cost, maintenance cost and operating expense. Equipment cost also includes the cost of equipment replacement throughout the life time of the system. The objectives of the financial analysis are to analyse lifetime energy savings in terms of the financial value of each solar cooling system investigated. All calculations were conducted for a project life time of 20 years.

The cooling technologies are compared based on UCC that represents the life cycle cost for one kWh of cooling, analogous to the levelised energy cost used in the analysis of electricity generation (Mokhtar et al., 2010) that were determined by using Eqs. (15)–(19).

$$UCC = \frac{ALCC\ (\$\ \mathrm{yr}^{-1})}{\text{Cooling supplied}\ (\mathrm{kWh_r\ yr}^{-1})} \tag{15}$$

$$ALCC = \frac{LCC}{Pa} \tag{16}$$

$$Pa = \left(\frac{1}{1+d}\right)\left(\left|\frac{1}{1+d}\right|^{t} - 1\right)\Big/\left(\frac{1}{1+d} - 1\right) \tag{17}$$

$$d = \left(\frac{1+D}{1+i}\right) - 1 \tag{18}$$

$$LCC = IC + \sum_{n=1}^{t} C_r \frac{1}{(1+d)^n} \tag{19}$$

where Pa is present worth factor, t is lifetime (year), d is the real discount rate, D is nominal discount rate, i is inflation rate, IC is initial cost of the system ($), and C_r is for each single future cost ($) to take into account all the operating cost over 20 years that was assumed to be constant for each year except replacement cost occurred. To carry out

Table 4
CDD for seven cities.

City	Jan	Feb	Mar	Apr	May	Jun	Jul	Aug	Sep	Oct	Nov	Dec
Darwin	124	129	121	127	126	78	52	83	100	140	159	167
Brisbane	42	35	29	5	1	1	0	5	8	8	15	42
Perth	69	68	45	14	2	0	0	0	9	15	28	55
Sydney	21	23	16	4	0	0	0	0	3	4	9	14
Adelaide	48	33	17	10	0	0	0	0	0	10	12	43
Canberra	11	15	4	0	0	0	0	0	0	0	9	9
Melbourne	16	39	7	1	0	0	0	0	0	2	5	13

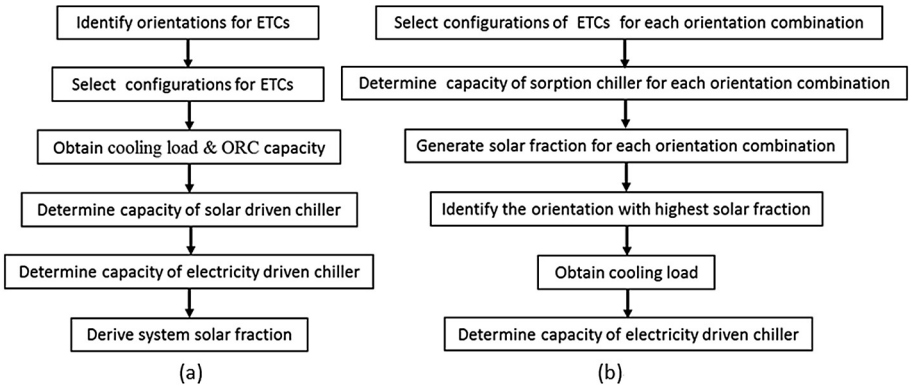

Fig. 13. Framework used for system sizing and performance assessment.

the financial analysis, some assumptions about costs have been made (Table 8) with real discount rate 8% (Harberger and Jenkins, 2015). The lifetime of PV panels and ETCs were assumed to be 30 and 15 years, respectively. The rest of the main components (ORCs, chillers and cooling towers) were assumed to have lifetime of 20 years. The unit cost of balance of plant (BOP) for the conventional, PV and solar thermal cooling systems were $285, $300 and $598, respectively. And the unit cost of engineering and installation of each of these systems were $124, $377 and $265, respectively (Kohlenbach and Dennis, 2010). Costs of cooling towers, ORCs and chillers of each component were gathered from the manufacturers. The maintenance cost is taken as a certain percentage of the initial capital cost. The assumed maintenance cost for solar technology with thermal output, solar technology with electric output, PV and cooling equipment is 1.5%, 2%, 1% and 2% respectively (Mokhtar et al., 2010). Electricity costs are provided in Table 8 with real escalation rate 3% (AEMO, 2012). The residual values of the systems were not considered in the analysis. The losses of efficiency in PV and ETC over time were neglected.

The total initial system cost, specific system cost, ALCC and UCC for conventional systems and the four solar cooling systems investigated in seven cities are presented in Table 9.

As expected, conventional cooling systems always have lower life cycle costs than solar cooling systems in each city, due to around 3 times lower capital cost than solar cooling systems. Fig. 14 shows the ranking of all the selected solar cooling options in this study. Three observations could be made from Fig. 14. First, for solar cooling systems, PV always has the lowest UCC although it has a slightly higher initial cost in Darwin. The relatively high initial cost in Darwin is offset by lower operational cost. This is contributed by PV system's relatively simple configuration, high COP of VCC chiller and the grid connection. Except in Darwin, PV systems can supply all electricity consumption in all other cities without utilising the full façade area that makes PV systems having very low operational costs. Secondly, in contrast, the single-stage absorption chiller is always the least economic system with the highest UCC regardless climate conditions. This is contributed by the both relatively high initial cost and operational cost. Thirdly, the cost difference between the ORC-VCC and adsorption system is very minor. The UCC of ORC-VCC system is only about 5% cheaper than adsorption system in seven cities. Although, ORC-VCC system has the lowest efficiency and most complicated configuration, it still could achieve the second-best financial performance due to longer operating period in subtropical and temperate climate conditions.

It should be noted that in Darwin, the variations of UCC among these solar cooling systems are very small. There is no particular solar cooling system having absolute economic advantage. This is caused by the whole-year long cooling period. The longer cooling period leads to more energy and financial savings achieved during life time. The savings are compensating the high initial costs of ORC-VCC and sorption cooling system.

However, the discrepancy is expanded with the decreased cooling

Table 6
System design parameters for seven cities.

Item	System	Darwin	Brisbane	Perth	Sydney	Adelaide	Canberra	Melbourne
Peak cooling load (kW_r)	Conventional	266	242	272	264	285	198	243
	PV	221	185	231	215	243	160	200
	ORC-VCC	218	180	228	208	230	152	176
	AD	218	180	228	208	230	152	176
	AB1	218	180	228	208	230	152	176
Annual total cooling (kWh_r)	Conventional	569,643	346,962	293,427	231,230	200,238	122,870	144,980
	PV	400,381	180,471	199,136	149,729	130,164	84,874	96,279
	ORC-VCC	417,585	166,757	188,673	151,174	116,419	69,732	78,246
	AD	417,585	166,131	182,016	146,014	112,256	65,344	78,184
	AB1	417,585	166,131	182,016	146,014	112,256	65,344	78,184
No. of ETCs in series on north, west	ORC-VCC	8,8	8,8	10,10	10,10	10,10	9,9	10,10
	AD	4,4	4,4	5,5	6,6	5,5	5,5	5,5
	AB1	3,3	2,2	4,4	4,4	4,4	4,4	4,4
Solar field area (m^2)	PV	480	340	368	382	254	170	226
	ETC	480	480	480	480	480	480	480
Capacity of solar thermal chiller (kW_r)	ORC-VCC	20	20	20	20	20	20	20
	AD	50	50	40	30	40	50	40
	AB1	60	60	50	50	50	40	50
Capacity of electricity chiller (kW_r)	ORC-VCC	218	176	210	203	220	152	168
	AD	218	163	203	184	220	152	168
	AB1	218	180	203	203	233	152	168
Capacity of ORC (kW)	ORC-VCC	14	14	10	11	11	12	10

Table 7
Annual electricity consumption (kWh_e).

System	Darwin	Brisbane	Perth	Sydney	Adelaide	Canberra	Melbourne
Conventional	169,885	95,227	81,513	60,774	55,678	35,021	41,512
PV	24,649	0	0	0	0	0	0
ORC-VCC	104,885	30,721	48,332	33,672	22,427	10,336	15,473
AD	135,358	47,134	57,453	47,155	32,448	25,134	26,722
AB1	142,235	51,412	60,485	45,267	34,386	19,960	22,794

demand in sub-topic and temperate climate condition zones. The PV system becomes much more competitive in terms of financial performance. This explains the energy saving from electricity and cooling generation in each system is insufficient to subsidise their capital investment, even though the ORC-VCC system is capable to operate through the whole year as long as the threshold solar radiation is achieved. Therefore, the selection of solar cooling system is not a sensitive factor in tropic climate zones if economic aspect is considered only. Please note that the degradation effects were excluded in the financial analysis. Although the absolute financial performance of each system could be affected by the degradation, this study is interested in the relative rankings of systems only which are expected not to be sensitive to the degradation effect.

6.2. Technical performance

To further compare these four systems, the SFs are shown in Table 10. As mentioned previously, the PV system can obtain 100% solar fraction in all cities expect in Darwin. In general, ORC-VCC system has higher SF compared to other sorption chillers, except in Darwin. It can achieve a solar fraction up to 32% in Brisbane with almost the same UCC as sorption systems. This is mainly due to feeding back excess electricity to the grid. Without this feature, ORC-VCC systems would be much less competitive because of the low efficiency of ORC. This is also the reason to explain the lowest SF (11%) achieved by the ORC-VCC system in Darwin. As a tropic city, the cooling season lasts the whole year; the whole system is running for cooling only. In contrast, under sub-tropic and temperate conditions, during non-cooling season, the ORC-VCC is the only operating solar driving system, which will increase annual energy saving potential dramatically. Meanwhile, it should be noted that the ORC industry is not fully mature at this stage and low-capacity systems are currently under development (Quoilin et al., 2013). There is a large potential for reduction in initial costs of ORC systems. Compared to single-stage absorption chillers, adsorption chillers always have lower costs but with similar levels of SF. Therefore, adsorption chiller systems would be a better choice than single-stage absorption chillers.

7. Conclusions

A preliminary system optimisation and comparative study were conducted for the four façade integrated solar cooling systems for a typical office building in Australian seven cities. The main objective of this investigation is to assess and compare the technical and financial performance of various façade integrated solar cooling technologies under different climate conditions. The method is based on assessing each solar cooling technology as a complete system constrained by climate and cooling demand as necessary conditions.

The assessment was done on the conventional system and pre-selected four solar cooling systems which can be built by using “off-the-shelf” components. The technologies were ranked from both technical and financial perspectives. Financial results indicated that at current conditions, solar cooling technology is still less cost competitive compared to conventional cooling systems (at least 50% higher than conventional system). Among the solar cooling systems, PV system is the most cost-effective one followed by ORC coupled with VCC chiller,

Table 8
Cost data assumptions applied.

Item	System	Darwin	Brisbane	Perth	Sydney	Adelaide	Canberra	Melbourne
Solar field ($ m^{-2})	PV	750 [1]	750	750	750	750	750	750
	ETC	314 [2]	314	314	314	314	314	314
Cooling tower ($ kWr^{-1}) [3]	Conventional	24	25	24	25	24	28	25
	PV	27	29	26	27	25	31	27
	ORC-VCC	28	28	26	26	26	30	28
	AD	27	27	25	27	25	27	27
	AB1	26	25	25	25	25	28	26
Solar thermal driven chiller ($ kW_r^{-1})	ORC-VCC	695	695	695	695	695	695	695
	AD [4]	616	579	616	673	616	579	616
	AB1 [5]	1505	1505	1751	1751	1751	2099	1751
Electricity driven chiller ($ kW_r^{-1}) [6]	Conventional	243	294	275	280	267	326	293
	PV	200	337	301	313	293	360	324
	ORC-VCC	168	345	317	322	312	369	352
	AD	168	357	322	338	309	369	352
	AB1	168	341	322	322	309	369	352
ORC ($ kW_m^{-1}) [7]	ORC-VCC	5000	4668	5000	4882	4882	4792	5000
Maintenance cost ($ kW_r^{-1})	Conventional	14	15	14	14	14	15	15
	PV	33	24	29	30	24	26	26
	ORC-VCC	34	37	33	34	33	40	40
	AD	35	38	33	34	33	42	42
	AB1	41	45	39	41	38	49	49
Business electricity price ($ kWh^{-1}) [8]	N/A	0.30	0.31	0.33	0.37	0.47	0.27	0.32

[1] (Nordin and Rahman, 2017); [2] (Steven, 2017); [3] (CTS, 2018); [4] (Khan, 2013); [5] (Jessica, 2017); [6] (Jones, 2017); [7] (Lemmens, 2015); (OTER, 2017).

Table 9
Initial and life cycle costs.

Item	System	Darwin	Brisbane	Perth	Sydney	Adelaide	Canberra	Melbourne
Initial cost ($)	Conventional	189,424	176,199	192,686	188,333	199,682	151,005	176,674
	PV	583,572	320,358	507,933	504,272	432,380	298,357	375,281
	ORC-VCC	491,888	451,479	483,815	469,043	490,258	414,412	431,049
	AD	442,109	398,971	443,645	418,277	455,187	372,423	392,079
	AB1	503,634	463,925	506,727	489,467	518,283	427,157	455,144
Specific cost ($ kWr^{-1})	Conventional	712	728	708	713	701	763	727
	PV	2641	1732	2199	2345	1779	1865	1876
	ORC-VCC	2256	2508	2122	2255	2132	2726	2449
	AD	2028	2217	1946	2011	1913	2450	2228
	AB1	2310	2577	2222	2353	2178	2811	2586
ALCC ($ a^{-1})	Conventional	78,192	52,362	49,921	42,664	42,394	29,761	34,995
	PV	74,757	37,135	58,351	57,861	49,959	34,539	43,357
	ORC-VCC	96,271	67,370	77,277	70,640	69,530	56,458	60,250
	AD	101,398	67,603	76,291	69,902	71,510	57,292	60,150
	AB1	111,125	76,906	84,961	77,964	77,881	62,295	66,561
UCC ($ kWh^{-1})	Conventional	0.14	0.15	0.17	0.18	0.21	0.22	0.24
	PV	0.21	0.24	0.29	0.39	0.38	0.41	0.45
	ORC-VCC	0.23	0.40	0.41	0.47	0.60	0.81	0.77
	AD	0.21	0.38	0.39	0.46	0.63	0.81	0.73
	AB1	0.23	0.44	0.43	51	0.70	0.91	0.82

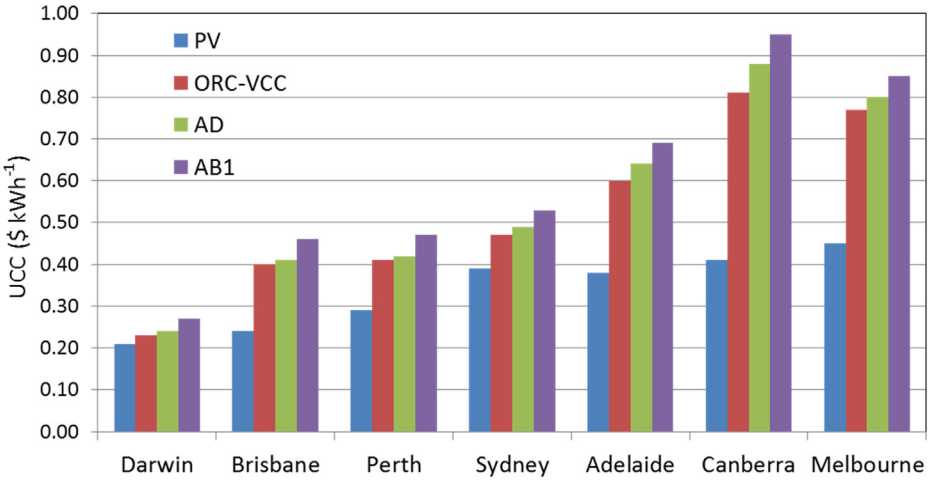

Fig. 14. UCC of façade integrated solar cooling systems.

Table 10
Solar fraction of façade integrated solar cooling systems.

System	Darwin	Brisbane	Perth	Sydney	Adelaide	Canberra	Melbourne
PV	60%	100%	100%	100%	100%	100%	100%
ORC-VCC	10%	32%	21%	23%	30%	27%	31%
AD	13%	28%	20%	20%	25%	20%	22%
AB1	14%	22%	20%	19%	25%	23%	22%

adsorption and single-stage absorption system. In tropic climate zone, this trend is not obvious. The single-stage absorption chiller system is only 21% high than the cheapest PV system. Therefore, the length of cooling season is a key factor for the system selection. In terms of system performance, PV system can provide the highest SF, followed by ORC coupled with VCC chiller, adsorption and single-stage absorption system.

Overall, based on the UCC and SF, the ranking order (first to fourth) of the four solar cooling system is:

- façade integrated semi-transparent PV (STPV) coupled with VCC chiller
- façade integrated ETC with combined ORC and VCC chiller
- façade integrated ETC with adsorption chiller
- façade integrated ETC with single-stage absorption chiller

Electricity generation and feeding back to the grid in ORC-VCC system is the key characteristic that makes it more competitive than other thermally driven systems, especially in sub-tropic and temperate climate zones. This conclusion not only provides a preliminary idea of technology selection for façade integrate solar cooling systems, it also proves the importance of development of ORC technology. Meanwhile, the framework described in this study provides a general method and can be applied to assess other potential systems and configurations. The conclusions may also be generalised for similar climate zones around the world.

Acknowledgements

This work was supported by the Australian Research Council Linkage Project funding [ARC-LP 110100429] and the Fundamental Research Funds for the Central Universities [2682018CX55]. The advice and funding support provided by Permasteelisa Group are also acknowledged.

References

ABCB, 2001. Discussion paper: definition of basic forms for representative buildings. Australi Australian Building Codes Board, Canberra.
AEMO, 2012. Economic outlook information paper: National electricity forecasting. Australian Energy Market Operator, Canberra.
AIRAH. 2018. https://www.airah.org.au/AIRAH/Navigation/Resources/SpecialInterestGroups/Solar_Cooling.aspx. (Accessed 6 January 2019).
Allouhi, A., Kousksou, T., Jamil, A., Bruel, P., Mourad, Y., Zeraouli, Y., 2015. Solar driven cooling systems: an updated review. Renew. Sustain. Energy Rev. 44 (44), 159–181.
Balaras, C.A., Grossman, G., Henning, H.-M., Infante Ferreira, C.A., Podesser, E., Wang, L., Wiemken, E., 2007. Solar air conditioning in Europe-an overview. Renew. Sustain. Energy Rev. 11 (2), 299–314.
Beccali, M., Cellura, M., Finocchiaro, P., Guarino, F., Longo, S., Nocke, B., 2014. Life cycle performance assessment of small solar thermal cooling systems and conventional plants assisted with photovoltaics. Sol. Energy 104 (104), 93–102.
Bellos, E., Tzivanidis, C., Antonopoulos, K.A., Gkinis, G., 2016. Thermal enhancement of solar parabolic trough collectors by using nanofluids and converging-diverging absorber tube. Renew. Energy 94, 213–222.
Bosanac, M., Nielsen, J.E., 1997. In situ check of collector array performance. Sol. Energy 59 (4), 135–142.
CTS, 2018. Cooling tower price list. http://www.coolingtowersystems.com/cooling_twr_price.php. (Accessed 10 February 2018).
Davis, M.W., Fanney, A.H., Dougherty, B.P., 2002. Evaluating building integrated photovoltaic performance models. In: the 29th IEEE Photovoltaic Specialists Conference. IEEE, New Orleans, pp. 1642–1645.
Delcroix, B., Kummert, M., Daoud, A., Hiller, M., 2012. Conduction transfer functions in TRNSYS multizone building model: current implementation, limitations and possible improvements,. the 38th IEEE Photovoltaic Specialists Conference. Austin.
Desideri, U., Proietti, S., Sdringola, P., 2009. Solar-powered cooling systems: technical and economic analysis on industrial refrigeration and air-conditioning applications. Appl. Energy 86 (9), 1376–1386.
Duffie, J.A., Beckman, W.A., 2013. Solar engineering of thermal processes. John Wiley & Sons Inc, Hoboken, NJ.
Eicker, U., Pietruschka, D., 2009. Design and performance of solar powered absorption cooling systems in office buildings. Energy Build. 41 (1), 81–91.
Eicker, U., Pietruschka, D., Schmitt, A., Haag, M., 2015. Comparison of photovoltaic and solar thermal cooling systems for office buildings in different climates. Sol. Energy 118, 243–255.
Fung, T.Y., Yang, H., 2008. Study on thermal performance of semi-transparent building-integrated photovoltaic glazings. Energy Build. 40 (3), 341–350.
Gan, G., 2009. Effect of air gap on the performance of building-integrated photovoltaics. Energy 34 (7), 913–921.
Geoscience Australia and ABARE, 2010. Australian Energy Resource Assessment. Canberra.
Guardo, A., Coussirat, M., Egusquiza, E., Alavedra, P., Castilla, R., 2009. A CFD approach to evaluate the influence of construction and operation parameters on the performance of active transparent façades in Mediterranean climates. Energy Build. 41 (5), 534–542.
Guiqiang, L., Gang, P., Yuehong, S., Yunyun, W., Jie, J., 2014. Design and investigation of a novel lens-walled compound parabolic concentrator with air gap. Appl. Energy 125, 21–27.
Harberger, A.C., Jenkins, G.P., 2015. Musings on the social discount rate. J. Benefit-Cost Anal. 6 (1), 6–32.
Hartmann, N., Glueck, C., Schmidt, F., 2011. Solar cooling for small office buildings: comparison of solar thermal and photovoltaic options for two different European climates. Renew. Energy 36 (5), 1329–1338.
Henning, H.M., 2007. Solar assisted air conditioning of buildings-an overview. Appl. Therm. Eng. 27 (10), 1734–1749.
Infield, D., Eicker, U., Fux, V., Mei, L., Schumacher, J., 2006. A simplified approach to thermal performance calculation for building integrated mechanically ventilated PV facades. Build. Environ. 41 (7), 893–901.
Jessica, B., 2017. pers. comm., 23 July.
Johnson Controls, Model YCWL Water-Cooled Scroll Liquid Chiller Style A. https://www.johnsoncontrols.com/hvac-equipment/chillers/ycwl-water-cooled-scroll-chiller. (Accessed 20 February 2018).
Jones, T., 2017. pers. comm., 10 July.
Khan, K., 2013. pers. comm., 26 July.
Kim, D., Ferreira, C., 2008. Solar refrigeration options–a state-of-the-art review. Int. J. Refrig 31 (1), 3–15.
King, D.L., Kratochvil, J.A., Boyson, W.E., 1997. Field experience with a new performance characterization procedure for photovoltaic arrays, the 2nd World Conference and Exhibition on Photovoltaic Solar Energy Conversion. Vienna.
King, D.L., Kratochvil, J.A., Boyson, W.E., 2004. Photovoltaic array performance model. Sandia National Laboratories, Albuquerque, NM.
Klein, S., Beckman, W., Mitchell, J., Duffie, J., Duffie, N., Freeman, T., Mitchell, J., Braun, J., Evans, B., Kummer, J., 2010. TRNSYS 17: a TRaNsient SYstem Simulation program. Solar Energy Laboratory, University of Wisconsin-Madison.
Koeppel, E.A., Klein, S.A., Mitchell, J.W., 1995. Commercial absorption chiller models for evaluation of control strategies. ASHRAE Trans.: Symposia 101 (1), 1175–1184.
Kohlenbach, P., Dennis, M., 2010. Solar cooling in Australia: the future of air-conditioning? Ecolibrium 10 (11), 32–38.
Koroneos, C., Nanaki, E., Xydis, G., 2010. Solar air conditioning systems and their applicability-an exergy approach. Resour. Conserv. Recycl. 55 (1), 74–82.
Lazzarin, R.M., Noro, M., 2018. Past, present, future of solar cooling: Technical and economical considerations. Sol. Energy.
Le, C., Bansal, P., Tedford, J., 2004. Energy saving strategies for a process multiple-chiller plant, Institute of Refrigeration, Heating and Air Conditioning Engineers Auckland.
Lemmens, S., 2015. A perspective on costs and cost estimation techniques for organic Rankine cycle systems. In: the 3rd International Seminar on ORC Power Systems. Brussels, Belgium, pp. 12-14.
Lu, L., Law, K.M., 2013. Overall energy performance of semi-transparent single-glazed photovoltaic (PV) window for a typical office in Hong Kong. Renew. Energy 49, 250–254.
Lu, Z.S., Wang, R.Z., Xia, Z.Z., Lu, X.R., Yang, C.B., Ma, Y.C., Ma, G.B., 2013. Study of a novel solar adsorption cooling system and a solar absorption cooling system with new CPC collectors. Renew. Energy 50 (3), 299–306.
Miyazaki, T., Akisawa, A., Kashiwagi, T., 2005. Energy savings of office buildings by the use of semi-transparent solar cells for windows. Renew. Energy 30 (3), 281–304.
Mokhtar, M., Ali, M.T., Bräuniger, S., Afshari, A., Sgouridis, S., Armstrong, P., Chiesa, M., 2010. Systematic comprehensive techno-economic assessment of solar cooling technologies using location-specific climate data. Appl. Energy 87 (12), 3766–3778.
Morrison, G., Litvak, A., 1999. Condensed solar Radiation database for Australia. Solar Thermal Energy Laboratory, University of New South Walse, Sydney.
Nordin, N., Rahman, H., 2017. Sizing and economic analysis of stand-alone photovoltaic system with hydrogen storage. In: IOP Conference Series: Earth and Environmental Science.
Obernberger, I., Thonhofer, P., Reisenhofer, E., 2002. Description and evaluation of the new 1,000 kWel Organic Rankine cycle process integrated in the biomass CHP plant in Lienz, Austria. Euroheat Power 10 (1), 18–25.
Otanicar, T., Taylor, R.A., Phelan, P.E., 2012. Prospects for solar cooling – An economic and environmental assessment. Sol. Energy 86 (5), 1287–1299.
OTER, 2017. Comparison of Australian Standing Offer Energy Prices August 2017. Office of the Tasmanian Economic Regulator, Hobart.
Qu, M., Yin, H., Archer, D.H., 2010. A solar thermal cooling and heating system for a building: experimental and model based performance analysis and design. Sol. Energy 84 (2), 166–182.
Quoilin, S., Broek, M.V.D., Declaye, S., Dewallef, P., Lemort, V., 2013. Techno-economic survey of organic Rankine cycle (ORC) systems. Renew. Sustain. Energy Rev. 22, 168–186.
Radhi, H., 2010. Energy analysis of façade-integrated photovoltaic systems applied to UAE commercial buildings. Sol. Energy 84 (12), 2009–2021.
Rahman, M.M., Rasul, M., Khan, M.M.K., 2010. Energy conservation measures in an institutional building in sub-tropical climate in Australia. Appl. Energy 87 (10), 2994–3004.
Raja, V.B., Shanmugam, V., 2012. A review and new approach to minimize the cost of solar assisted absorption cooling system. Renew. Sustain. Energy Rev. 16 (9), 6725–6731.
Saghafifar, M., Gadalla, M., 2016. Performance assessment of integrated PV/T and solid desiccant air-conditioning systems for cooling buildings using Maisotsenko cooling cycle. Sol. Energy 127, 79–95.
Song, J.-H., An, Y.-S., Kim, S.-G., Lee, S.-J., Yoon, J.-H., Choung, Y.-K., 2008. Power output analysis of transparent thin-film module in building integrated photovoltaic system (BIPV). Energy Build. 40 (11), 2067–2075.
SPF, 2004. Collector Test Reports. Institute of Solar Research, Cologne.
Steven, H., 2017. pers. comm., 10 July.
Superchill. http://www.superchill.com.au/catalogue.shtml. (Accessed 12 July 2018).
The Government of Western Australia, 2011. Commercial building energy efficiency. http://www.finance.wa.gov.au/cms/content.aspx?id=14160. (Accessed 12 July 2013).
Ullah, K.R., Saidur, R., Ping, H.W., Akikur, R.K., Shuvo, N.H., 2013. A review of solar thermal refrigeration and cooling methods. Renew. Sustain. Energy Rev. 24 (10), 499–513.
Wang, H., Peterson, R., Herron, T., 2011. Design study of configurations on system COP for a combined ORC (organic Rankine cycle) and VCC (vapor compression cycle). Energy 36 (8), 4809–4820.
Wang, X., Chen, D., Ren, Z., 2010. Assessment of climate change impact on residential building heating and cooling energy requirement in Australia. Build. Environ. 45 (7), 1663–1682.
Wang, Y., Tian, W., Ren, J., Zhu, L., Wang, Q., 2006. Influence of a building's integrated-photovoltaics on heating and cooling loads. Appl. Energy 83 (9), 989–1003.
Weber, C., Berger, M., Mehling, F., Heinrich, A., Núñez, T., 2014. Solar cooling with water–ammonia absorption chillers and concentrating solar collector – Operational experience. Int. J. Refrig. 39 (1), 57–76.
Wu, D., Aye, L., Mendis, P., Ngo, T., 2013. Financial analysis of solar cooling systems in Australia. In: the Australian Solar Cooling 2013 Conference. Sydney.
Wu, D., Aye, L., Mendis, P., Ngo, T., 2017. Optimisation and financial analysis of an organic Rankine cycle cooling system driven by facade integrated solar collectors. Appl. Energy 185, 172–182.
Xuan, Q., Li, G., Pei, G., Ji, J., Su, Y., Zhao, B., 2017. Optimization design and performance analysis of a novel asymmetric compound parabolic concentrator with rotation angle for building application. Sol. Energy 158, 808–818.
Zeyghami, M., Goswami, D.Y., Stefanakos, E., 2015. A review of solar thermo-mechanical refrigeration and cooling methods. Renew. Sustain. Energy Rev. 51, 1428–1445.